EUROPEAN ORGANIZATION FOR NUCLEAR RESEARCH

CERN - PS DIVISION

CERN/PS 96-13 (AR)

REVIEW OF RECENT WORK ON ELECTRON COOLING AT LEAR

J. Bosser

(On behalf of the CERN-LEAR team and of the Russian Collaboration)

Abstract

The Low-Energy Antiproton Ring (LEAR) is expected to be used as an accumulator in the frame work of the LHC lead-ion project. This implies at first that the electron-cooled ions have a lifetime which is longer than the stacking time. On the other hand, in order to improve the electron-cooling time we expect to make use of large electron beam intensities, of the order of 0.5 A, at relativistic parameter $\beta = v/c = 0.09$. With such constraints the electron beam density is rather large so the induced space-charge forces become detrimental to the cooling process itself. A neutralization of the electron beam, which aims to reduce the effects of the space-charge forces, is therefore desirable. This paper describes the measurements made on the cooling and lifetimes and on the neutralization technique implemented on the LEAR electron cooler.

Paper presented at the 31st Eloisatron Workshop on Crystalline Beams and Related Issues, Erice, 11-21 November 1995

Geneva, Switzerland
1/4/96

1 INTRODUCTION

The Low-Energy Antiproton Ring (LEAR) is expected to be used as a lead-ion accumulator in the framework of the LHC project [1]. Multistacking and efficient electron cooling should allow one to obtain the required beam intensity and the requested small emittances.

The main LEAR and Electron Cooler parameters are given in Table 1.

Table 1. LEAR and Electron Cooler main parameters for the lead-ion project.

LEAR for lead ions	
Energy	4.2 MeV/u
Velocity factor β	0.094
Ion charge state	52^+, 53^+, or 54^+
Ion beam current	20–25 μAe
Corresponding number of ions	$2.3\text{–}2.8 \cdot 10^6$ ions/μs
Stacking process time [s]	$\simeq 2$
Vacuum pressure [torr]	$2 \cdot 10^{-11}$ (85% H_2 and He)
Electron Cooler	
Cooling length/circumferene = η_{ecool}	0.02
Electron beam radius a [cm]	2.5
Beam pipe radius b [cm]	5 or 7
Typical electron current I_e [A]	0.2 [0.4]
Electron density in cooling section $n_e = I_e/e\pi a^2\beta c$ [m^{-3}]	$1.13 \cdot 10^{14} \cdot I_e$
Effective electron density per turn $n_{\mathrm{eff}} = \eta_{\mathrm{ecool}} \cdot n_e$ [m^{-3}]	$2.25 \cdot 10^{12} \cdot I_e$
Typical longitudinal B-field in cooler B [T]	0.06
Lattice functions at the cooler $\beta_H = 1.9$ m, $\beta_V = 5.3$ m, $D = 3.6$ m	

In the framework of our project it is fundamental to have a good understanding of:

- the ion beam lifetime with and without electron cooling,
- the dense electron beam space-charge effects on its transverse velocity.

As a consequence we have measured the lead-ion beam lifetimes, under different conditions, together with the cooling time. We have also implemented and tested an electron beam neutralization technique intended to reduce the space-charge effects (tests have mainly been done with protons at various energies).

The outcome of these two types of experiments will be briefly reported hereafter. For more details the reader is invited to consult Refs. [2]–[6].

2 LEAD-ION LIFE AND COOLING TIMES

The ion lifetime 'τ' is expressed by the following equation:

$$\frac{1}{\tau}[\mathrm{s}^{-1}] = \frac{1}{\tau_{\mathrm{vac}}} + \frac{1}{\tau_{\mathrm{rec}}}$$

where:

τ_{vac} : is the lifetime due to the effects resulting from the interactions of the ions with the residual gas molecules alone. It depends of course on the residual gas composition which has to be measured.

τ_{rec} : is the lifetime resulting from the different types of recombination of the positive lead ions with the co-moving electrons of the cooler. The recombinations may be of the radiative or dielectronic type but we were not able to distinguish between them.

2.1 LEAR vacuum conditions

A careful analysis of the LEAR residual gas partial pressure is made at four significant locations of the ring. Table 2 shows the measurements made at the time of the actual experiments on life and cooling time. From theoretical formulae we deduce the expected lifetime which is $\tau_{vac} = 17.6\ s = 1/\langle t_{life} \rangle = 1/0.057$. This agreement can be considered as coincidental; nevertheless the gas composition must be known with accuracy prior to any statement on the lifetime and also to compare the results of different experiments.

Table 2. Estimate of LEAR vacuum conditions and calculated lifetime [7].

		Analyser										
		102		204[a]		303		304			Ring averages	
		Length [m]										
		50		50		4		4				
Rest gas	Lifetime for 10^{-12} torr	P[b]	$\langle P \rangle$[c]	P	$\langle P \rangle$	P	$\langle P \rangle$	P	$\langle P \rangle$	$\langle P \rangle$ ring	Rel. $\langle P \rangle$ ring	$1/\langle t_{life} \rangle$
H_2	625	16.00	10.19	5.10	3.25	16.00	0.81	6.10	0.31	14.56	0.73	0.023
He	624	0.60	0.38	1.30	0.83	3.10	0.16	9.40	0.48	1.85	0.09	0.003
CH_4	126	0.40	0.25	1.60	1.02	1.10	0.06	1.10	0.06	1.39	0.07	0.011
H_2O	129	0.72	0.46	1.40	0.89	0.00	0.00	1.10	0.06	1.41	0.07	0.011
N_2	92	0.00	0.00	0.00	0.00	0.00	0.00	2.00	0.10	0.10	0.01	0.001
CO	92	0.20	0.13	0.28	0.18	0.85	0.04	0.00	0.00	0.35	0.02	0.004
Ar	76	0.00	0.00	0.21	0.13	0.00	0.00	0.17	0.01	0.14	0.01	0.002
CO_2	59	0.00	0.00	0.16	0.10	0.00	0.00	0.13	0.01	0.11	0.01	0.002
Sum										**19.91**		**0.057**

[a] Note: 50 m is 10 m for sector 2 and 40 m for sector 4 where vacuum is four times worse.
[b] P = partial physical pressure in 10^{-12} torr.
[c] $\langle P \rangle$ = contribution of this section to the average pressure of the ring.

2.2 Measurement of the lifetime

2.2.1 Method of measurement

Owing to the small circulating beam intensity we were not able to estimate the lifetime with the help of the classical current transformer. We therefore used the signal of a longitudinal Schottky pickup processed by a spectrum analyser. In our case $\Delta p/p$ is rather large so that the integrated Schottky noise power $S^2(t)$ is proportional the circulating unbunched ion-beam intensity. Data from the spectrum analyser are acquired by a laptop computer which does the relevant computations, namely the suppression of the electronic noise and the curve fittings.

2.2.2 Results

A plot of the inverse cooling time: $1/\tau$ [s^{-1}], as a function of the cooler current I_e [mA], is given by Fig. 1 for three different ion charge states (namely Pb^{52+}, Pb^{53+}, and Pb^{54+}).

Once the common vacuum inverse lifetime $1/\tau_{vac} = 1/20$ [s] has been subtracted one gets Fig. 2 where the three curves cross at the origin. It appears clearly that lifetimes of Pb^{52+} and Pb^{54+} are about the same and significantly larger than that of Pb^{53+} ions.

From the slope of the curves on Fig. 2 one can deduce the rate coefficient α defined by

$$\alpha = \left(\frac{1}{\tau}\right) / n_{\text{eff}} \ [\text{cm}^3\text{s}^{-1}]$$

$$\alpha = \frac{1}{\tau} \cdot \frac{1}{2.25 \cdot 10^6} \cdot \frac{1}{I_e} \quad \text{for our case .}$$

According to our measurements:

$$\alpha\,[\text{Pb}^{52+}] = 11 \cdot 10^{-8}, \quad \alpha\,[\text{Pb}^{53+}] = 60 \cdot 10^{-8}, \quad \alpha\,[\text{Pb}^{54+}] = 9 \cdot 10^{-8} \ .$$

We have no explanation for such differences of the rate coefficient with respect to the charge state number. The choice of Pb^{52+} or Pb^{54+} ions looks therefore for the time being, to be the most favourable since the linac feeding LEAR can provide the three types of ions with almost the same intensity.

Even with $I_e = 0.5$ A a lifetime of about six seconds looks quite comfortable when compared to the stacking time.

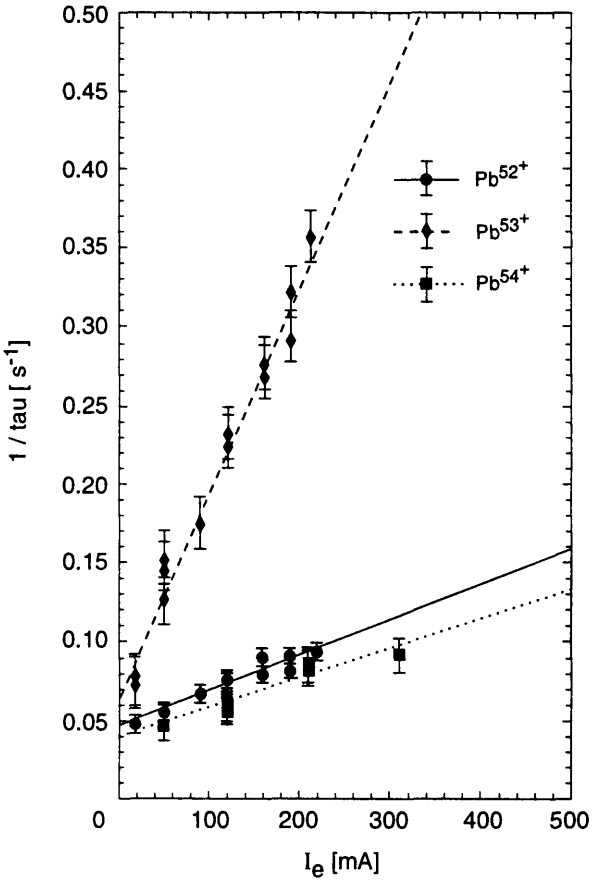

Figure 1: Dependence of the overall inverse beam lifetime $1/\tau$ [s^{-1}] as a function of the electron cooling current I_e [mA], for the three lead-ion species.

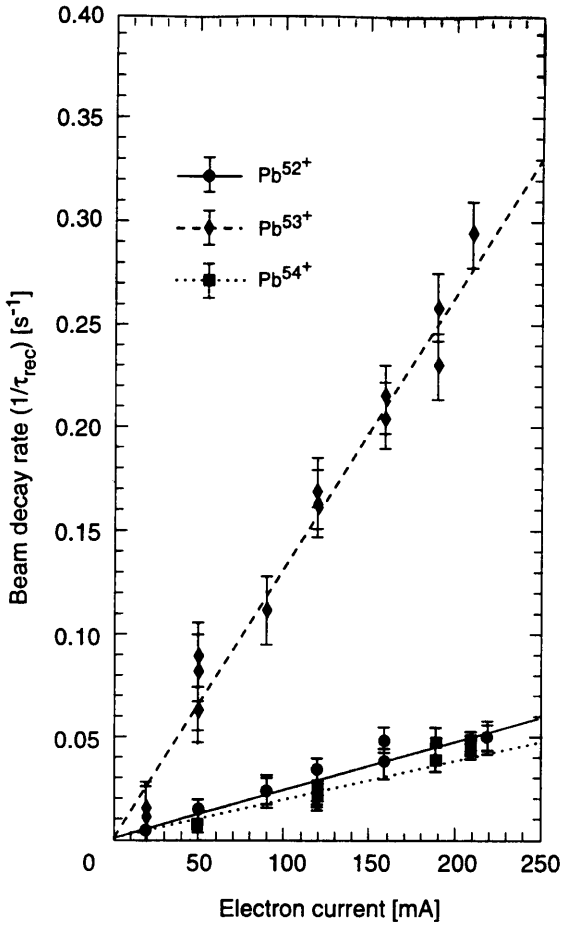

Figure 2: Dependence of the inverse beam recombination lifetime $1/\tau_{\rm rec}$ as a function of the electron cooling current $I_{\rm e}$ [mA], for the three lead-ion species.

2.3 Cooling time measurement

2.3.1 Method of measurement

The longitudinal cooling time from $\Delta p/p = 10^{-3}$ to $\Delta p/p = 10^{-4}$ is about 50 ms when $I_{\rm e} = 120$ mA. It is measured, as usual, from the longitudinal Schottky pickup signal.

The transverse cooling times (H and V) are measured by horizontal and vertical ionization monitors. The electrons coming out of the micro-channel plate are collected by metallic strips distant by 1 mm one from the other and integrated at fixed time intervals. The signals are processed by a microprocessor which computes the major parameters, of the transverse distribution, versus time.

Figure 3 is an example of such a measurement in the horizontal plane for $I_{\rm e} = 120$ mA. One determines a cooling time from a uniform ion distribution (over the machine acceptance estimated as $A_{\rm H} = 150\pi$ mm $\cdot$ mrad), at injection, to an almost Gaussian distribution, with final r.m.s. emittance area

$$\epsilon = \pi \cdot \sigma^2/\beta_{\rm H} \sim \frac{2\ \text{mm}^2}{\beta_{\rm H}} \cdot \pi = 2 \cdot \pi \cdot 10^{-6}\ [\text{m}]\ ,$$

in about 300 ms. In the vertical plane we get almost the same results.

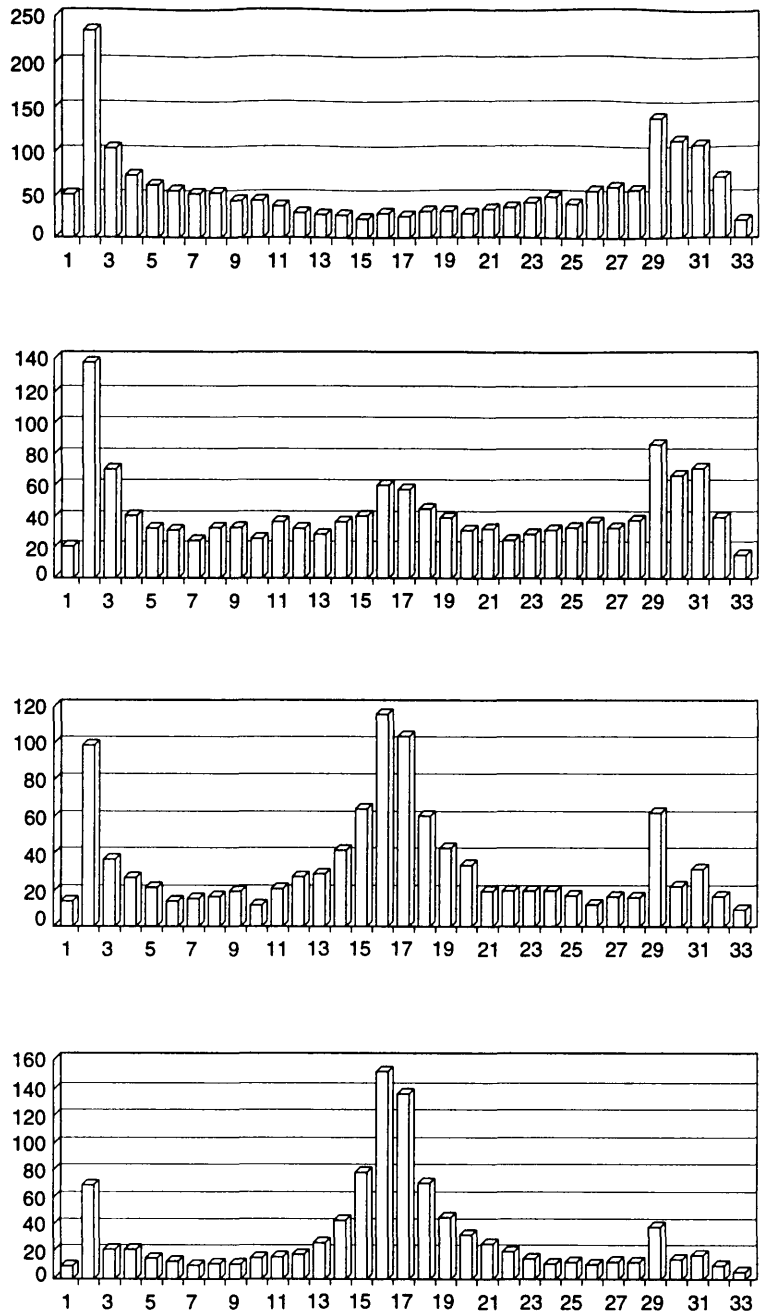

Figure 3: Horizontal beam profile measured by the ionization profile monitor. The time interval between each measurement is 100 ms. The top measurement corresponds to 0 s while the bottom one is at $t = 300$ ms. Horizontally the distance between the strips is 1 mm.

3 NEUTRALIZATION OF THE COOLER ELECTRON BEAM

3.1 Aim

The electron beam space-charge potential, U_{sp}, with respect to the beam pipe, of radius b, at ground potential, is a function of the radius r, as expressed by:

$$U_{\mathrm{sp}}(r) = -\frac{30 I_{\mathrm{e}}(1-\eta)}{\beta} \cdot \begin{cases} \left(1 + 2\ln\left(\frac{b}{a}\right) - \frac{r^2}{a^2}\right) & \text{for } 0 \le r \le a \\ 2\ln\left(\frac{b}{r}\right) & \text{for } a \le r \le b \end{cases}$$

where η, the neutralization factor, is equal to $Z_{\mathrm{i}} n_{\mathrm{i}} / n_{\mathrm{e}}$ with $Z_{\mathrm{i}} n_{\mathrm{i}}$ [m^{-3}] the density of the ions, of charge Z_{i}, which are considered uniformly stored within the electron beam volume.

The longitudinal magnetic field B is adjusted so as to, at least, limit the electron beam radius increase as a consequence of the radial electrical force $F_r = e \cdot (\partial U_{sp}/\partial r)$.

With a dense electron beam, i.e. the electron density $n_e = (I_e/e\pi a^2 \beta c)$ is large, two main issues of the space-charge effect, may be considered.

First the electron kinetic energy E_c is a function of the radius r since:

$$\begin{aligned} E_c = (\gamma - 1) m_e c^2 &= e[U_{cathode} + U_{space-charge}] \\ E_c(r) &= e[U_c + U_{sp}(r)] \simeq \frac{1}{2} m_e v_{\parallel}^2(r) \end{aligned}$$

with $v_{\parallel}$ the longitudinal component of the electron velocity. The electron beam has thus a longitudinal velocity distribution as represented by Fig. 4. Together with the electron longitudinal velocity distribution we have to consider the corresponding ion velocity distribution $v_{i\parallel}(r)$ which depends on the dispersion D [m] since $r_i = D \cdot (\Delta p/p) = D \cdot \gamma^2 (\Delta v_{i\parallel}/v_{i\parallel})$ as also represented in Fig. 4 where we also show the effects of the ion transverse r.m.s. beam width $\sigma = \sqrt{\epsilon_{H,V} \cdot \beta_{H,V}}$. Depending on D the curves representing the electron on the ion velocity may intersect at a radius $r_i = a_1 \neq 0$.

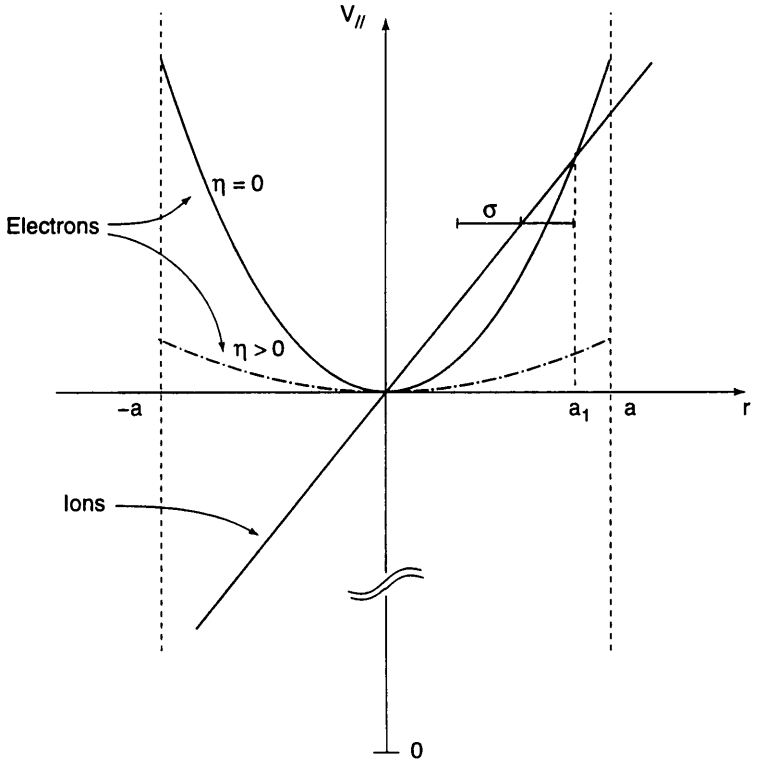

Figure 4: Electron and ion longitudinal velocities versus the horizontal position x for two neutralization factors $\eta (= 0$ or $> 0)$. The electron beam radius is denoted by 'a'. We consider having adjusted U_c, as we do during normal operation, so as to always keep the electron velocity equal to the ion nominal velocity whatever the value of the neutralization coefficient (η).

The cooling force f_{cool} is proportional to $(v_e - v_i)/|v_e - v_i|^3$. Therefore an ion with radius $r_i > a_1$ such that $v_{i\parallel} < v_{e\parallel}$ will be subject to heating. Hence small $\eta (< 0.2)$ and large $n_e (> 10^{13}\,\mathrm{m}^{-3})$ may induce heating (rather than cooling) on the circulating ions. Any attempt to increase η and therefore to neutralize the electron beam, will reduce effects of this nuisance (see Fig. 4 for $\eta > 0$).

As a second consequence of dense electron beams we have to consider that F_r will induce an azimuthal transverse velocity, also named drift velocity, v_d, expressed by:

$$v_d = \frac{F_r}{w_H} \quad \text{where} \quad w_H = \frac{eB}{m_e} .$$

This velocity adds quadratically to the electron nominal transverse velocity which thus, for large densities n_e, will be significantly increased. Since the electron cooling process is based on the fact that the electrons have to be very cold, a way to reduce v_d is to reduce F_r and therefore to neutralize the electron beam ($F_r(\eta = 1) = 0$).

3.2 Principle (Fig. 5)

For the purpose of neutralization we have installed two sets of electrodes, one El_g at the gun level, the other, El_c, at the collector level. Each electrode consists of two metallic half-cylinders separated by a glass insulator (small conductivity). Each metallic plate is polarized by independent positive (versus ground) voltages: $U_{eli}(0 \leq U_{eli} \leq 6$ kV, $i = 1, ..., 4)$.

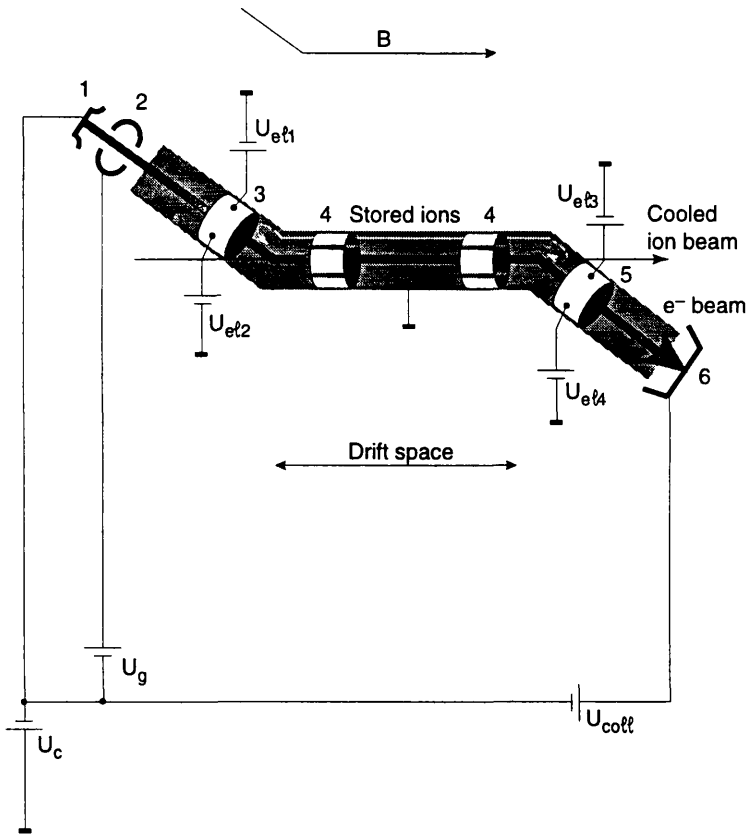

Figure 5: Principle of neutralization.
1 Cathode + gun; 2 Control grid; 3 Neutralization 'gun' electrode El_g; 4 Horizontal and vertical pickups; 5 Neutralization 'collector' electrode El_c; 6 Collector.

On their way from the gun to the collector the energetic electrons will ionize the residual gas molecules which are almost at rest. The positively ionized ions will drift slowly, in the longitudinal magnetic field B, toward El_c or El_g were they are reflected. The slow electrons will also reach the electrodes of El_c or El_g where they are collected. The density n_i [m^{-3}] of the stored ions, between the neutralization electrodes, will thus

increase with time until it reaches its asymptotic value. The neutralization factor η is defined by $\eta = (Z_i n_i / n_e)$, $(0 \leq \eta \leq 1)$.

It must be emphasized that, on our electron cooler the beam pipe diameter b_1, between the gun and El_g and El_c and the collector, is 100 mm while, between El_g and El_c, b_2 is equal to 140 mm. This discontinuity will induce different space-charge potentials such that, even with no potential on El_g and El_c, $\Delta U_{sp} = (30 I_e/\beta) \cdot 2\ln(b_2/b_1)$ which has the same physical effect as that induced by an artificial neutralization by the help of the U_{eli}'s. Thus these discontinuities in the beam pipe diameters induce a 'natural neutralization' [8].

The main problem of the neutralization process is that under some conditions, namely when I_e exceeds a given threshold, η becomes unstable i.e. part or all of the stored ions are suddenly expelled. We therefore have developed some diagnostics to measure dynamically η and to observe its instability. A so-called 'shaker' has been implemented which aims to suppress the above-mentioned neutralization instabilities.

3.3 Measurement of the neutralization factor η

We mainly use two methods, one measuring the cooled ion revolution frequency (and thereby the ion velocity) and the other making use of the electron time of flight (TOF) between El_g and El_c.

3.3.1 Revolution frequency measurement

The electron beam velocity at $r = 0$, which also fixes the cooled ion beam mean velocity $\langle v_i \rangle$ is given by:

$$\langle \beta_i \rangle \cdot c = \langle v_i \rangle = v_{e_\parallel}(r = 0) \simeq \left\{ \frac{2e}{m} \left(U_c - \frac{90 I_e}{\langle \beta_i \rangle} (1 - \eta) \right) \right\}^{1/2}$$

where U_c is the cathode potential (Fig. 5). An increase of η implies therefore a decrease of U_c in order to keep $\langle v_i \rangle$ or the ion revolution frequency fr at their nominal values since

$$\frac{\Delta fr}{fr} = \left(1 - \frac{\gamma^2}{\gamma_t^2} \right) \frac{\Delta \beta}{\beta} \simeq \frac{\Delta \beta}{\beta} \text{ and } \gamma_t^2 \gg 1$$

in LEAR.

As a consequence the cathode corrections ΔU_c we have to apply to the cathode in order to keep the ion revolution constant do permit us to retrieve $\Delta\eta$. At full neutralization $(\eta = 1)$ any change of I_e has no influence on $\langle v_i \rangle$.

This method is used as a reference intended to calibrate the TOF technique we are going to describe now.

3.3.2 Time-Of-Flight method (TOF)

The principle described by Fig. 6 is based on the fact that the propagation of a density modulation imposed on the electron beam depends, to the first order, primarily on the electron mean velocity and so on the neutralization factor η. For that purpose the primary electron beam longitudinal density is weakly modulated by a sinusoidal signal applied on El_g. This excitation signal is delivered by a network analyser at a frequency f close to 300 MHz. The modulated signal is detected by El_c which is at an electrical distance 'L' from El_g.

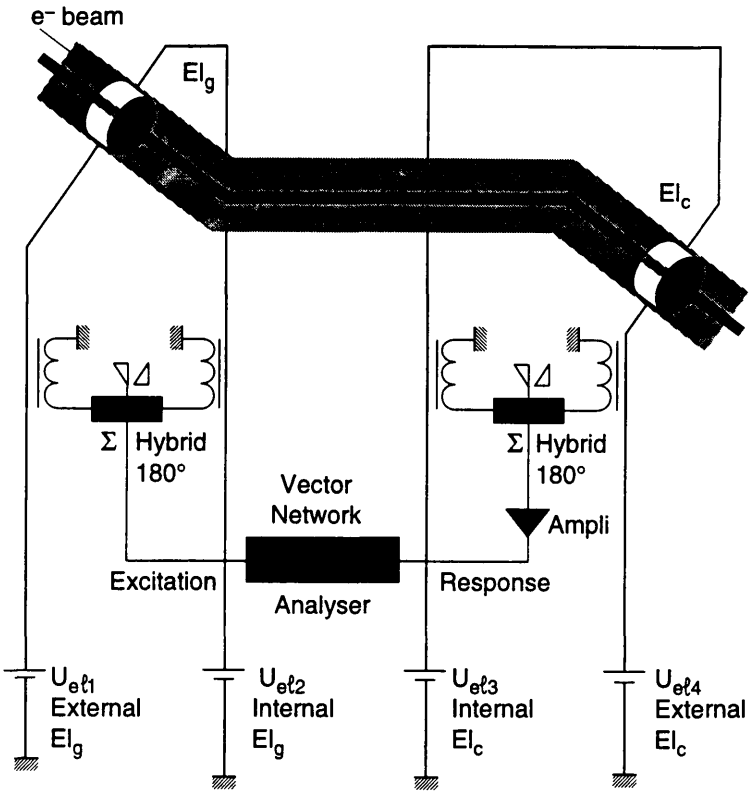

Figure 6: Principle of the TOF method.
El_g Neutralization electrode gun; El_c Neutralization electrode collector.

The difference in phase between the excitation and the detected signals, as measured by the analyser, is expressed by

$$\phi(El_c) - \phi(El_g) = -\frac{(2\pi f)}{v_{e_\parallel}} L$$

or

$$\Delta\phi \simeq \frac{(2\pi f)}{v_{e_\parallel}} L \cdot \frac{\Delta v_e}{v_{e_\parallel}}(\eta) \, .$$

From the measurement of $\Delta\phi$ one can easily retrieve $\Delta\eta$. An example of such a measurement is given by Fig. 7. At the time when the neutralization electrodes are polarized one observes a small but sharp change of $\Delta\phi$ followed by a much larger amplitude variation during a much longer time which corresponds to the overall neutralization time (about 3 s on Fig. 7). The short initial $\Delta\phi$ is thought to be due to the capture of stored electrons by the neutralization electrodes at the time when the positive neutralization voltages U_{el_i} are applied.

A comparison of the two methods gives comparable estimates of η within an uncertainty of 20% which can be explained by the measurement described in the next paragraph.

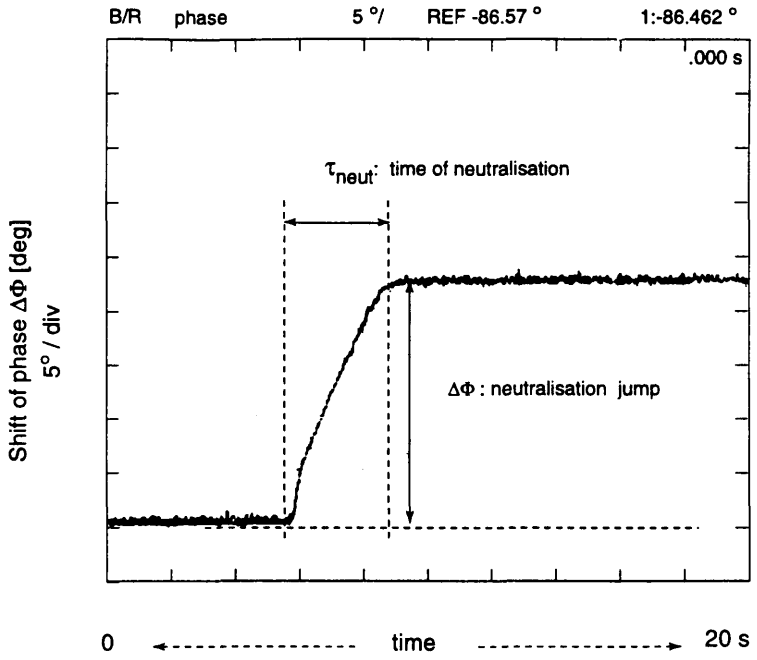

Figure 7: TOF measurement. Plot of $\Delta\phi$ [deg] as a function of time t [s].

3.3.3 Distribution of η

The cooled ion beam has a diameter of a few millimetres and can be used as a probe of the electron beam. It is then possible to use the LEAR orbit correctors in order to displace the ion beam transversally within the electron beam and to measure the corresponding ion revolution frequency changes as a function of the ion beam radial position. Such measurements are shown in Fig. 8.

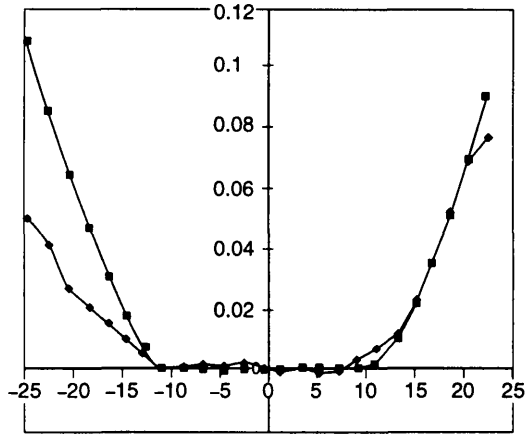

Figure 8: Neutralization distributions. Horizontal axis: position [mm]. Vertical axis: frequency shift [kHz].

It appears clearly that, by polarizing the neutralization electrodes, the electron beam is fully neutralized over an interval of about ± 1 cm around the centre. Taking into account the finite dimension of the ion beam, the measurement for $|r| \geq 15$–20 mm must be used with care since the electron beam radius 'a' is equal to 25 mm.

3.4 Instabilities of the neutralization factor: cures

Instabilities of η are observed mainly when the primary electron beam intensity exceeds a given threshold. One observes jumps of the energy which follow from a sudden expulsion of the stored ions which participate in the neutralization process. This effect is clearly revealed by the time-of-flight method (see 3.3.2) or when looking at the signals induced on the position pickup electrodes [6]. These instabilities happen sometimes when we operate under natural neutralization conditions (see 3.2) i.e. when all the El_g and El_c electrodes are at ground potential.

One of the simplest way to suppress these instabilities is to make use of a so-called 'shaker'. The principle is shown in the lower part of Fig. 9. A low-voltage (few tenths of a volt) sinewave, with a frequency of a few 100 kHz, is applied transversally on any of the position pickup electrodes in the cooling section. This arrangement damps any instability while reducing slightly the stable value of η. Referring to the top part of Fig. 9, which shows the network analyser (measuring the TOF) display, one sees on the left the phase (see 3.3.2) or 'η' instabilities while the right part shows the stabilizing effect of the shaker for different voltage levels.

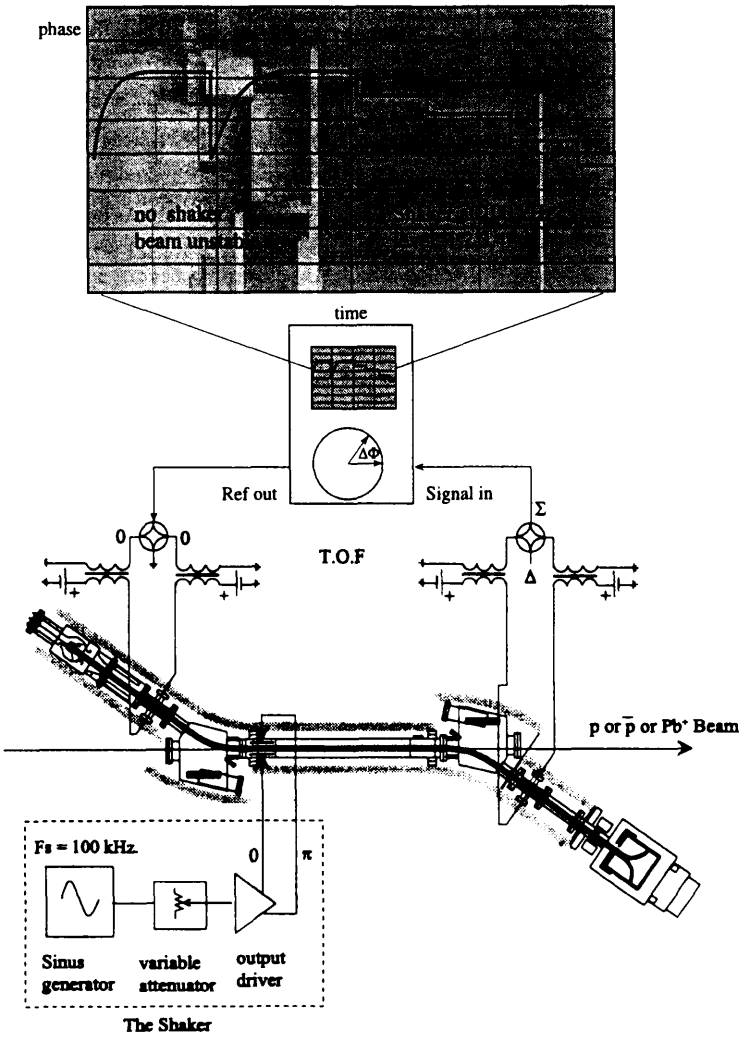

Figure 9: Principle of the 'shaker'. Top: display of the network analyser phase (or TOF) measurement. The left part shows an unstable neutralization while the right part shows stable neutralization for different shaker voltage amplitudes.

4 CONCLUSIONS

Experiments done on LEAR showed that Pb^{52+} and Pb^{54+} are good candidates as far as the lifetime and the transverse cooling time are concerned. A future increase of the electron cooler intensity from 0.12 to 0.5 A and a lengthening of the drift space (η_{ecool} increased from 0.02 to 0.04) should permit one to lower the transverse cooling time from 0.3 to 0.1 s.

The neutralization process has been partially understood and mastered. Future improvements, like that aiming to clear the electrons which are reflected by the collector, and also the use of a quadrupolar type 'shaker' are under way. We also foresee getting rid of the natural neutralization by equalizing the beam pipe diameters along the electron beam trajectory.

References

[1] P. Lefèvre and D. Möhl, Lead ion accumulation scheme for LHC, CERN/PS/DI/Note 95–09, LHC Note 257;
P. Lefèvre and D. Möhl, A low energy accumulation ring of ions for LHC, CERN/PS/DI/Note 93–62, LHC Note 259.

[2] S. Baird, J. Bosser, C. Carli, M. Chanel, P. Lefèvre, R. Ley, R. Maccaferri, S. Maury, I. Meshkov, D. Möhl, G. Molinari, F. Motsch, H. Mulder, G. Tranquille and F. Varenne, Beam lifetime tests for Pb^{52+}, Pb^{53+} and Pb^{54+} ions subject to electron cooling in LEAR (performed in June 1995), PS/AR/Note 95–12.

[3] S. Baird, J. Bosser, C. Carli, M. Chanel, P. Lefèvre, R. Ley, R. Maccaferri, S. Maury, I. Meshkov, D. Möhl, G. Molinari, F. Motsch, H. Mulder, G. Tranquille and F. Varenne, Measurement of the lifetime of Pb^{52+}, Pb^{53+} and Pb^{54+} beams at 4.2 MeV per nucleon subject to electron cooling, *Phys. Lett.* **B361** (1995) 184.

[4] J. Bosser, F. Caspers, M. Chanel, R. Ley, R. Maccaferri, S. Maury, I. Meshkov, G. Molinari, V. Polyakov, A. Smirnov, O. Stepashkin, E. Syresin, G. Tranquille and F. Varenne, Neutralisation of the lear electron-cooling beam: experimental results, Part. Acc. Conf., Dallas, 1995, CERN/PS 95–17 (AR).

[5] J. Bosser, S. Maury, I. Meshkov, D. Möhl, E. Mustafin, E. Syresin, F. Varenne and P. Zenkerich, Stability conditions for a neutralised electron cooling beam, Part. Acc. Conf., Dallas, 1995, CERN/PS 95–16 (AR).

[6] F. Varenne, Neutralisation de la charge d'espace du faisceau d'électrons du refroidisseur électronique de LEAR (in French), Thesis, Clermont-Ferrand University, November 1995.

[7] B. Franzke, Vacuum requirements for heavy ion synchrotrons, Proc. Part. Acc. Conf., *IEEE Trans. Nucl. Sci.* **NS-28** (1981) 2116.

[8] G. Tranquille, Suppression of the natural neutralisation of the electron beam space charge via polarised tubes, PS/OP/Note 95–47.